Supplementary data for

Zhang *et al.* Sirtuin 2 deficiency aggravates ageing-induced vascular remodelling in humans and mice

Supplementary Method

Human samples

Human aortic samples were obtained as described previously.[1] The human abdominal aortic aneurysm (AAA) samples were obtained from patients undergoing open surgical repair. The AAA was diagnosed with ultrasound scanning. The control samples were obtained from the adjacent nonaneurysmal aortic segments. All protocols using human aortic samples were approved by the Ethical Committee of the Chinese Academy of Medical Sciences and Peking Union Medical College.

Immunoprecipitation and western blot

Cultured cells were lysed with immunoprecipitation (IP) buffer (Beyotime Biotechnology, P0013) supplemented with a protease inhibitor cocktail (Bimake, B14001) and phosphatase inhibitor (Bimake, B15001). After sonication and centrifugation at 13,000 × *g* for 20 min, the lysates were precleared and incubated with the indicated primary antibodies overnight at 4°C and then incubated with Protein A/G PLUS-Agarose (Santa Cruz, sc-2003) for 2 h at 4°C. The beads were then washed five times with IP buffer and protein samples were harvested. For the western blot protein preparation, protein was extracted with RIPA lysis buffer (Beyotime Biotechnology, P0013B) supplemented with a protease inhibitor cocktail (Bimake, B14001) and phosphatase inhibitor (Bimake, B15001). The homogenates were sonicated and centrifuged at 4°C for 15 min, and the supernatants were used for western blot. Protein aliquots (20–50 μg) were separated by sodium dodecyl sulfate–polyacrylamide gel electrophoresis and transferred to a polyvinyldene fluoride membrane (Millipore). After blocking with 5% skim milk in Tris-buffered saline with Tween-20, the membranes were incubated with primary antibodies overnight at 4°C. Subsequently, the membrane was incubated with a horseradish peroxidase–conjugated secondary antibody (ZSGB-BIO, ZB2301/ZB2305) and exposed to Pierce ECL Western Blot Substrate (Thermo, 32106) for the detection of protein expression. The primary antibodies used in this study are listed below: Shc (BD Bioscience, 610878), p-p66^{Shc} (phospho-S36; Abcam, ab54518), SIRT2 (Sigma, S8447; Proteintech, 19655-1-AP), glyceraldehyde-3-phosphate dehydrogenase (GAPDH; Proteintech, 60004-1-Ig), HA tag (Proteintech, 51064-2-AP), Myc tag (Santa Cruz, sc-40), histone 3 (Abcam, ab1791), H3K18ac (ABclonal, A7257), H3K18cr (PTM Biolabs, PTM-517), pan-benzoyllysine (PTM Biolabs, PTM-762), MMP2 (Proteintech, 10373-2-AP), MMP9 (Proteintech, 10375-2-AP), c-Src (Proteintech, 60315-1-Ig), p-c-Src (ABclonal, AP0452), 3-Nitrotyrosine (PTM Biolab, PTM-752), SOD2 (Millipore, 06-984), Catalase (Santa, sc-271803). Mouse monoclonal Ac-p66^{Shc}K81 antibody was generated by Dia-an (Wuhan, China) and provided by Prof. Yongzhang Luo (Tsinghua University); this antibody was described in a previous study.[2] For the western blot post-IP assay, IPKine™ HRP Mouse Anti-Rabbit IgG LCS (Abbkine, A25022) and IPKine™ HRP Goat Anti-Mouse IgG LCS (Abbkine, A25012) were used as secondary antibodies.

Quantitative real-time polymerase chain reaction

To test the mRNA levels of the targeted genes, total RNA was extracted from the aortas using TRIzol reagent (Invitrogen, 15596026). Total RNA (1 μg) was subjected to cDNA synthesis using a First Strand cDNA Synthesis Kit (New England Biolabs, M0277). Quantitative real-time PCR (qRT-PCR) was performed to detect the mRNA levels of the target genes using AceQ qPCR SYBR Green Master Mix (Vazyme, Q111-02). The thermocycling conditions used for qRT-PCR amplification were as follows: 5 min at 95°C for pre-denaturation and 40 consecutive cycles of amplification (10 s at 95°C for denaturation, 30 s at 60°C for annealing and extension). *GAPDH* (*Gapdh*) was used to normalise the mRNA levels using the 2^-ΔΔCt method. The primers used in this study are listed in Table S1.

Functional analysis

The pulse wave velocity and constriction relaxation of the aortas were analysed as described previously.[1,3,4]

Histopathological analysis

For histological analysis, the mouse aortas were fixed in 4% paraformaldehyde. Fixed aortas were embedded in paraffin, cut into 5 μm sections, and stained using a haematoxylin-eosin kit (Servicebio, G1005). Images were analysed using Image Pro Plus 6.0.

Histochemical staining and ROS measurement

Immunofluorescence staining was performed to analyse SIRT2 expression in the aortas. Aortas from young and aged mice were fixed with 4% paraformaldehyde in phosphate-buffered saline for 24 h and embedded in OCT. Sections (7 μm) were prepared and blocked in 10% foetal bovine serum (FBS) in phosphate-buffered saline at room temperature for 1 h. The slides were then incubated with primary antibodies at 4°C overnight, followed by incubation with fluorescently coupled secondary antibodies for 45 min, and DAPI/Hoechst for 10 min at room temperature. Immunofluorescence analysis of cultured cells was performed. The following primary antibodies were used: SIRT2 (Sigma, S8447; Proteintech, 19655-1-AP), alpha-smooth muscle actin (Sigma-Aldrich, A5691), CD11c (Servicebio, GB11059), Ly6G (Servicebio, GB11229), F4/80 (Servicebio, GB113373), Arg-1 (Servicebio, GB11285), CD206 (Servicebio, GB113497), CD86 (BIOSS, bs-1035R), iNOS (Proteintech,18985-1-AP). The fluorescently conjugated secondary antibodies used were donkey anti-mouse immunoglobulin G (H+L), Alexa Fluor® 488 (ThermoFisher, R37114), and donkey anti-rabbit immunoglobulin G (H+L), Alexa Fluor® 594 (ThermoFisher, R37119). The results were analysed using Image Pro Plus software (Media Cybernetics) after adjusting the scale.

Immunohistochemical staining was performed to monitor collagen, MCP-1, matrix metalloproteins (MMPs), immune cells (CD45), and macromolecular oxidation in aortic tissues, according to a previously described method.[4-6] Collagen I (GB114197), Collagen III (GB111629), MCP-1 (GB11199), MMP2 (GB11130), MMP9 (GB11132), and CD45 (GB113885) antibodies were purchased from Servicebio. 3-Nitrotyrosine antibody (bs-8551R) and 4-Hydroxynonenal antibody (bs-6313R) were purchased from BIOSS. 8-Oxoguanine antibody (MAB3560) was purchased from Sigma-Aldrich. Paraffin sections (5 μm) were subjected to immunohistochemical analysis as described previously[7]. The results were analysed using the Image Pro Plus software (Media Cybernetics) after adjusting the scale. Elastin van Gieson staining was performed to analyse elastin fibres as we described previously[1]. Immune cells were quantified based on a method described previously.[8]

Dihydroethidium (DHE) and MitoSOX staining were performed to monitor the levels of total superoxide and mROS, DHE, and MitoSOX staining were performed respectively. Briefly, frozen aortas were cut into 7 μm sections. The sections and cultured cells were stained with 5 μM DHE (Invitrogen, D11347) or MitoSOX (Invitrogen, M36008) at 37°C for 30 min and measured by fluorescence microscopy. The results were analysed using the Image Pro Plus software (Media Cybernetics) after adjusting the scale.

Vascular cell preparation and flow cytometry

The aortic was stripped of the outer membrane, then minced, and digested with mixed enzymes solution (125 U/ml collagenase type XI, 60 U/ml hyaluronidase type 1, 60 U/ml DNase I, and 450 U/ml collagenase type I; all from Sigma-Aldrich) to obtain the single cell suspensions. Next, a 6-colour panel flow cytometry was performed to analyse macrophages, as described previously.[9,10] The antibodies Fixable Viability Stain 780 (565388), rat anti-mouse CD45 V500 (561487), rat Anti-CD11b FITC (553310), rat anti-mouse F4/80 BV421 (565411), rat anti-mouse CD86 PE (553692), and rat anti-mouse CD206 Alexa Fluor® 647 (565250) were purchased from BD Bioscience. The samples were analysed using the BD FACS Aria III and the FCS EXPRESS software 7.0 (De Novo Software).

SIRT2 activity measurement

SIRT2 activity was analysed as described previously.[11] Briefly, SIRT2 protein was purified by immunoprecipitation using excessive SIRT2 antibodies (Sigma, S8447) from young and aged aortas of WT and *Sirt2*-KO mice. The enzymatic activity of SIRT2 was determined using a CycLex® SIRT2 Deacetylase Fluorometric Assay Kit ver. 2 (Medical & Biological Laboratories, CY-1152V2) according to the manufacturer's instructions.

Cell isolation, culture, and transfection

Mouse aortic smooth muscle cells (ASMCs) were isolated from mouse aortas.[12] The cells were maintained in Dulbecco's modified Eagle's medium containing 15% FBS (Sigma, 12003C).[1] Human ASMCs were purchased from ScienCell (6110), and cultured in Smooth Muscle Cell Medium (ScienCell,1101) with 10% FBS[1]. For knockdown of *p66^{Shc}* in ASMCs, cells were transfected with si-NC or si-*p66^{Shc}* (5'-UGAGUCUCUGUCAUCGCUG[dT][dT]-3')[13] using the Lipofectamine™ RNAiMAX kit (Thermo Fisher, 13778075).

Adenovirus generation and infection

To overexpress p66^{Shc} or SIRT2, an adenovirus was used. The adenovirus expressing HA-tagged SIRT2 (Ad-HA-SIRT2) was described previously.[11] the p66^{Shc} construct was cloned into the pAdTrack-CMV plasmid to generate the pAdTrack-*Myc-p66^{Shc}* plasmid. The pAdTrack-*Myc-p66^{Shc}* plasmid was linearised using the restriction endonuclease *Pme I (NEB)*. The linearised DNA construct was transformed into pAdEasy-1 electrocompetent BJ5183 cells and clones with successful homologous recombination were verified. Next, the plasmids were extracted and linearised using restriction endonuclease *Pac I (NEB).* The linearised DNA product was transfected into HEK293A cells using VigoFect (Vigorous Biotechnology, T001) to produce an adenovirus expressing Myc-tagged p66^{Shc} (Ad-Myc-p66^{Shc}).

Cell death and proliferation assay

ASMCs were cultured and treated with the SIRT2 inhibitor, AGK2 (10 μM), for 24 h. The cells were then subjected to apoptosis analysis with fluorescein (FITC) TUNEL Cell Apoptosis

Detection Kit (Servicebio, G1501). For the cell proliferation assay, cells were cultured for 0, 24, 48, or 96 h in the presence or absence of the SIRT2 inhibitor AGK2 (10 μM). Cell counts were analysed using the Cell Counting Kit-8(CCK-8) kit (Servicebio, G4103).

Co-expression network analysis

The gene expression matrix (transcripts per million) of 6,074 human blood vessels was downloaded from the Genotype-Tissue Expression website (http://xena.ucsc.edu/public/). The gene expression matrix of ten mouse blood vessels was downloaded from the GEO database (GSE145972). We applied the z-score normalised gene expression matrix for 14,915 genes of human blood vessels and 19,398 genes of mouse blood vessels and built a Coexpression network by weighted gene co-expression network analysis (WGCNA)(v1.70.3),[14,15] by fitting a scale-free topology and applying a soft threshold power of 6 into an unsigned network model. 82 and 187 modules were identified in the human and mouse blood vessels, respectively. Pathway enrichment analysis of SIRT2-coexpressed genes was conducted and visualised using the R package "clusterProfiler" (v3.18.1). To examine whether SIRT2-coexpressed genes were associated with ages in humans, we calculated the eigengene of the SIRT2 module by the "moduleEigengenes" function and identified its significance across different ages by the Kruskal–Wallis with Dunn's *post hoc* test.

The predictive power of SIRT2-coexpressed genes in aortic diseases

Gene expression matrices for aortic diseases were downloaded from the GEO database (GSE140947 and GSE57691). To assign pathway activity estimates of SIRT2-coexpressed genes to individual samples, gene set variation analysis (GSVA) algorithm was implemented in the R package GSVA (v1.38.2).[16] The pathway activity of SIRT2-coexpressed genes in predicting aortic diseases was evaluated and visualised by R package "pROC" (v1.17.0) and "ggsci"(v2.9).

Single-cell RNA-seq data processing

Single-cell count matrices were downloaded from the GEO database (GSE155468) and loaded into R package Seurat (v 4.0.1). Cells with less than 200 genes, more than 4,000 genes, or more than 5% mitochondrial gene ratio were regarded as low-quality cells and were thus filtered. After data scaling and principal component analysis, cell clustering was conducted using the "FindClusters" function with the first 25 principal components. Cell annotations were adopted from previous annotations (GSE155468). Cell clusters were visualised with the "VlnPlot" function.

Transcriptome analysis

Total RNAs from the aortas of aged WT and *Sirt2*-KO mice (n=3) were subjected to bulk RNA-seq for transcriptome analysis. We used DESeq2 and two other well-established methods (limma[17] and edgeR[18]) to identify differentially expressed genes between WT and *Sirt2*-KO aorta samples. Based on this analysis, 844 genes were recognised as commonly upregulated genes resulting from the three methods ($|\log_2 FC| \geq 0.5$, adjusted $p < 0.05$). Gene Ontology pathway annotation and enrichment analyses were performed using the web tool ToppGene Suite (toppgene.cchmc.org) and visualised using the web tool Omicshare (www.omicshare.com). RNA-seq data from this study were deposited in the Gene Expression Omnibus database under accession number GSE199682.

Human plasma level of SIRT2

The plasma SIRT2 level across the lifespan was analysed using a public proteome dataset, which involved 2,925 plasma proteins from 4,263 young adults to nonagenarians (18–95 years old).[19] The graph showing circulating SIRT2 protein level was generated using the web tool: https://twc-stanford.shinyapps.io/aging_plasma_proteome/).

References

1. Chen H-Z, Wang F, Gao P, Pei J-F, Liu Y, Xu T-T*, et al.* Age-associated Sirtuin 1 reduction in vascular smooth muscle links vascular senescence and inflammation to abdominal aortic aneurysm. *Circ Res* 2016;**119**:1076-1088. doi: https://doi.org/10.1161/circresaha.116.308895
2. Jiang Y, Luo Z, Gong Y, Fu Y, Luo Y. NAD^+ supplementation limits triple-negative breast cancer metastasis via SIRT1-$P66^{Shc}$ signaling. *Oncogene* 2023;**42**:808-824. doi: https://doi.org/10.1038/s41388-023-02592-y
3. Wan YZ, Gao P, Zhou S, Zhang ZQ, Hao DL, Lian LS*, et al.* SIRT1-mediated epigenetic downregulation of plasminogen activator inhibitor-1 prevents vascular endothelial replicative senescence. *Aging Cell* 2014;**13**:890-899. doi: https://doi.org/10.1111/acel.12247
4. Zhang Y, Tang X, Wang Z, Wang L, Chen Z, Qian J*, et al.* The chemokine CCL17 is a novel therapeutic target for cardiovascular aging. *Signal Transduct Target Ther* 2023;**8**:157. doi: https://doi.org/10.1038/s41392-023-01363-1
5. Fukuda D, Aikawa E, Swirski FK, Novobrantseva TI, Kotelianski V, Gorgun CZ*, et al.* Notch ligand Delta-like 4 blockade attenuates atherosclerosis and metabolic disorders. *Proc Natl Acad Sci U S A* 2012;**109**:E1868-E1877. doi: https://doi.org/10.1073/pnas.1116889109
6. He C, Li H, Viollet B, Zou M-H, Xie Z. AMPK suppresses vascular inflammation in vivo by inhibiting signal transducer and activator of transcription-1. *Diabetes* 2015;**64**:4285-4297. doi: https://doi.org/10.2337/db15-0107
7. Liu Y, Wang TT, Zhang R, Fu WY, Wang X, Wang F*, et al.* Calorie restriction protects against experimental abdominal aortic aneurysms in mice. *J Exp Med* 2016;**213**:2473-2488. doi: https://doi.org/10.1084/jem.20151794
8. Mueller PA, Zhu L, Tavori H, Huynh K, Giunzioni I, Stafford JM*, et al.* Deletion of macrophage low-density lipoprotein receptor-related protein 1 (LRP1) accelerates atherosclerosis regression and increases C-C chemokine receptor type 7 (CCR7) expression in plaque macrophages. *Circulation* 2018;**138**:1850-1863. doi: https://doi.org/10.1161/circulationaha.117.031702
9. Zhang Y, Ye Y, Tang X, Wang H, Tanaka T, Tian R*, et al.* CCL17 acts as a novel therapeutic target in pathological cardiac hypertrophy and heart failure. *J Exp Med* 2022;**219**:e20200418. doi: https://doi.org/10.1084/jem.20200418
10. Lin Q-Y, Bai J, Zhang Y-L, Li H-H. Integrin CD11b contributes to hypertension and vascular dysfunction through mediating macrophage adhesion and migration. *Hypertension* 2023;**80**:57-69. doi: https://doi.org/10.1161/HYPERTENSIONAHA.122.20328
11. Tang X, Chen XF, Wang NY, Wang XM, Liang ST, Zheng W*, et al.* SIRT2 acts as a cardioprotective deacetylase in pathological cardiac hypertrophy. *Circulation* 2017;**136**:2051-2067. doi: https://doi.org/10.1161/CIRCULATIONAHA.117.028728
12. Kwartler CS, Zhou P, Kuang S-Q, Duan X-Y, Gong L, Milewicz DM. Vascular smooth muscle cell isolation and culture from mouse aorta. *Bio-protocol* 2016;**6**:e2045. doi: https://doi.org/10.21769/BioProtoc.2045

13. Spescha RD, Klohs J, Semerano A, Giacalone G, Derungs RS, Reiner MF*, et al.* Post-ischaemic silencing of $p66^{Shc}$ reduces ischaemia/reperfusion brain injury and its expression correlates to clinical outcome in stroke. *Eur Heart J* 2015;**36**:1590-1600. doi: https://doi.org/10.1093/eurheartj/ehv140
14. Langfelder P, Horvath S. WGCNA: an R package for weighted correlation network analysis. *BMC Bioinformatics* 2008;**9**:559. doi: https://doi.org/10.1186/1471-2105-9-559
15. Bottomly D, Long N, Schultz AR, Kurtz SE, Tognon CE, Johnson K*, et al.* Integrative analysis of drug response and clinical outcome in acute myeloid leukemia. *Cancer Cell* 2022;**40**:850-864. doi: https://doi.org/10.1016/j.ccell.2022.07.002
16. Hänzelmann S, Castelo R, Guinney J. GSVA: gene set variation analysis for microarray and RNA-seq data. *BMC Bioinformatics* 2013;**14**:7. doi: https://doi.org/10.1186/1471-2105-14-7
17. Ritchie ME, Phipson B, Wu D, Hu Y, Law CW, Shi W*, et al.* limma powers differential expression analyses for RNA-sequencing and microarray studies. *Nucleic Acids Research* 2015;**43**:e47-e47. doi: https://doi.org/10.1093/nar/gkv007
18. Robinson MD, McCarthy DJ, Smyth GK. edgeR: a Bioconductor package for differential expression analysis of digital gene expression data. *Bioinformatics* 2009;**26**:139-140. doi: https://doi.org/10.1093/bioinformatics/btp616
19. Lehallier B, Gate D, Schaum N, Nanasi T, Lee SE, Yousef H*, et al.* Undulating changes in human plasma proteome profiles across the lifespan. *Nat Med* 2019;**25**:1843-1850. doi: https://doi.org/10.1038/s41591-019-0673-2

Supplementary Table 1. Quantitative real-time polymerase chain reaction primers used in this study

Gene symbol	Forward primer (5'-3')	Reverse primer (5'-3')
h*SIRT1*	CCCTCAAAGTAAGACCAGTAGC	CACAGTCTCCAAGAAGCTCTAC
h*SIRT2*	ACGCTGTCGCAGAGTCAT	CGCTCCAGG GTATCTATGTT
h*SIRT3*	AGAAGAGATGCGGGACCTTG	GGTCCATCAAGCCTAGAGCAG
h*SIRT4*	GGCAGGAATCTCCACCGAAT	GCACTCCGGACAAAATCACC
h*SIRT5*	AGAGAGCTCGCCCACTGTGATTTA	AGGGTCCCTGGAAATGAAACCTGA
h*SIRT6*	AGTCTTCCAGTGTGGTGTTCC	TCCATGGTCCAGACTCCGT
h*SIRT7*	GGTGGAGCGGGAATAGTCAG	CTGGGATAGACGCTGCACAT
h*GAPDH*	GAAGGTGAAGGTCGGAGTCAAC	CAGAGTTAAAAGCAGCCCTGGT
m*Gapdh*	CAGCCTCGTCCCGTAGACA	CAACAATCTCCACTTTGCCACT
m*Sirt1*	AGAACCACCAAAGCGGAAA	TCCCACAGGAGACAGAAACC
m*Sirt2*	AGCCAACCATCTGCCACTAC	CCAGCCCATCGTGTATTCTT
m*Sirt3*	TGCTACTCATCTTGGGACCT	CACCAGCCTTTCCACACC
m*Sirt4*	GAGCAACTGGGAGAGACTGG	ACAGCACGGGACCTGAAA
m*Sirt5*	CGCTGGAGGTTACTGGAGA	CGTCAATGTTCTGGGTGATG
m*Sirt6*	CATGGGCTTCCTCAGCTTC	AACGAGTCCTCCCAGTCCA
m*Sirt7*	AGCCTACCCTCACCCACA	CGCTCAGTCACATCAAACAC

Supplementary Figures and Legends

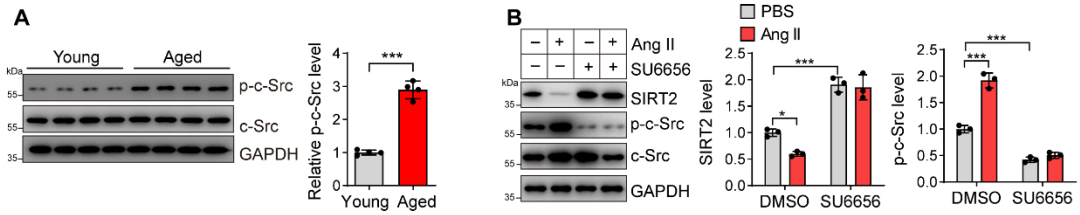

Supplementary Figure 1. c-Src regulates SIRT2 protein level in vascular cells. (A) c-Src protein level and phosphorylated level in young and aged mouse aortas (n=4). (B) Inhibition of c-Src with SU6656 (5 μM) inhibits decline in SIRT2 protein level induced by angiotensin II (1 μM) in aortic vascular smooth muscle cells (n=3). Statistical analyses were performed using unpaired Student's *t* test (A) and one-way ANOVA with Bonferroni *post hoc* test (B). **p*<0.05, ****p*<0.001.

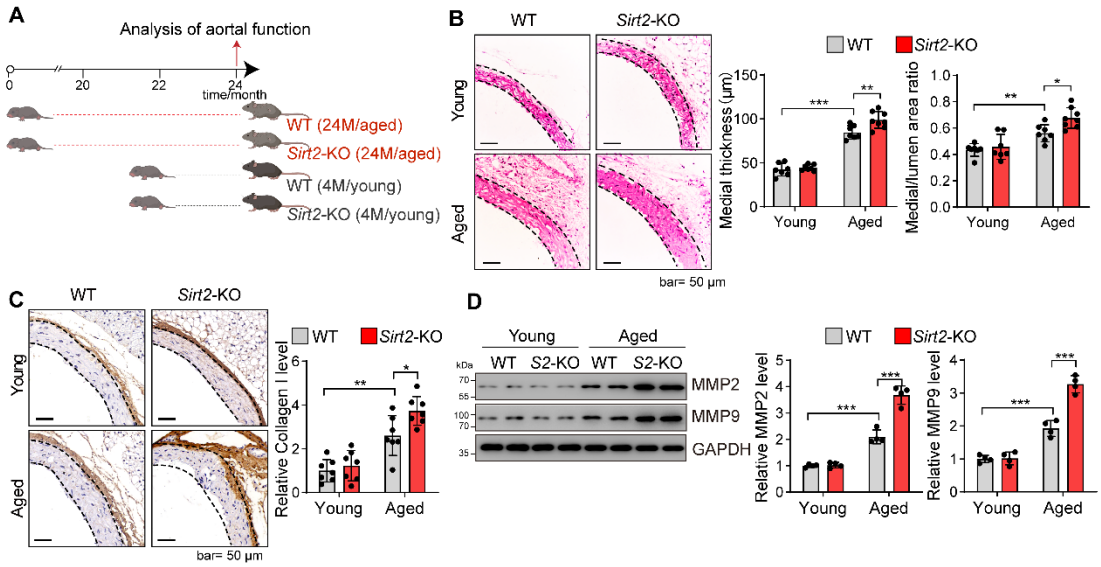

Supplementary Figure 2. *Sirt2* deficiency promotes ageing-induced vascular remodelling. (A) Experimental design. (B) Haematoxylin-eosin staining of the abdominal aortas was performed, and the medial thickness and the ratio of the media area to vessel lumen were quantified (n=7-8). (C) Immunohistochemical staining of Collagen I in the thoracic aorta. Representative images and quantitative results are shown (n=7). (D) Western blot analysis of MMP2 and MMP9 expression in aged aortas. Representative blots and quantitative results are shown (n=4). *S2*-KO=*Sirt2*-KO. Statistical analyses were performed using one-way ANOVA with Bonferroni *post hoc* test. **p*<0.05, ***p*<0.01, ****p*<0.001. MMP, matrix metalloproteinase.

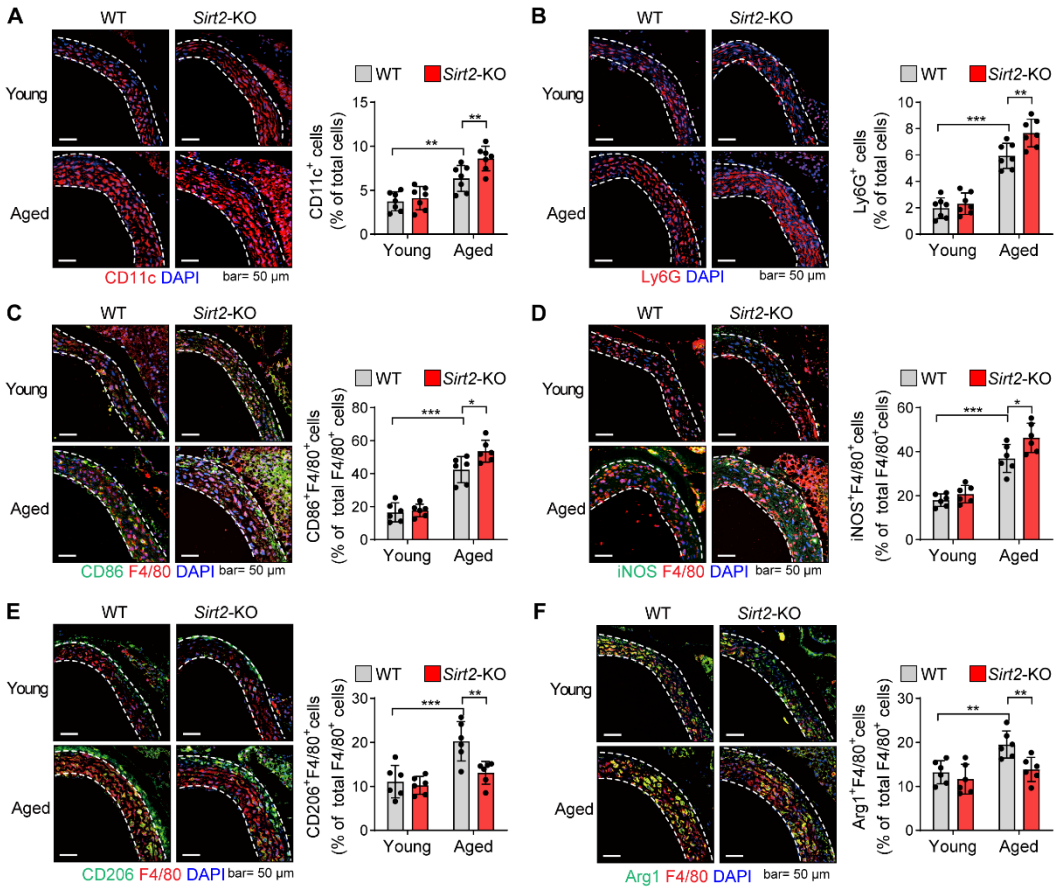

Supplementary Figure 3. SIRT2 regulates inflammation in aged aortas. (A) *Sirt2* deficiency promotes dendritic cell ($CD11c^+$) infiltration in aged aortas. Representative images and quantitative results are shown (n=7). (B) *Sirt2* deficiency promotes neutrophils ($Ly6G^+$) infiltration in aged aortas. Representative images and quantitative results are shown (n=7). (C-D) *Sirt2* deficiency promotes pro-inflammatory M1 macrophage ($CD86^+F4/80^+$ and $iNOS^+F4/80^+$) polarisation in aged aortas. Representative images and quantitative results are shown (n=6). (E-F) *Sirt2* deficiency reduces anti-inflammatory M2 macrophage ($CD206^+F4/80^+$ and $Arg1^+F4/80^+$) polarisation in aged aortas. Representative images and quantitative results are shown (n=6). Statistical analyses were performed using one-way ANOVA with Bonferroni *post hoc* test. **p*<0.05, ***p*<0.01, ****p*<0.001.

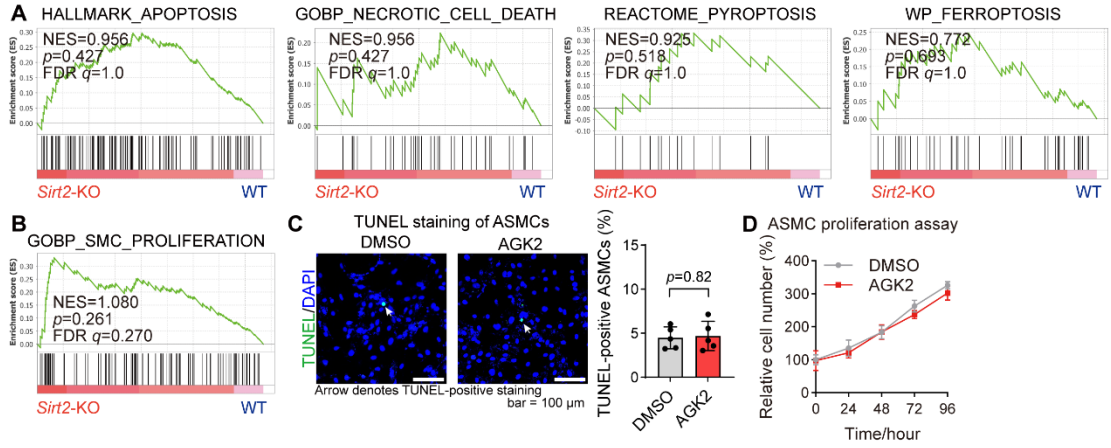

Supplementary Figure 4. SIRT2 does not affect vascular cell death and proliferation. (A) *Sirt2* knockout (*Sirt2*-KO) does not affect cell death signals in aged aortas. Gene set enrichment analysis was performed to analyse the enrichment of apoptosis, necrosis, pyroptosis, and ferroptosis signals in aged aortas from wild-type and *Sirt2*-KO mice. (B) Gene sent enrichment analysis revealing that *Sirt2* knockout does not affect SMC proliferation signal in aged aortas. (C) SIRT2 inhibition does not affect human aortic smooth muscle cell death. The cells were treated with SIRT2 inhibitor AGK2 (10 μM) or control dimethyl sulfoxide (DMSO) for 24 h, cell death was analysed by terminal deoxynucleotidyl transferase dUTP nick end labelling (TUNEL) staining. Representative images and quantitative results are shown (n=5). Statistical analysis was performed using unpaired Student's *t* test. (D) SIRT2 inhibition does not affect human aortic smooth muscle cell proliferation. The cells were treated with SIRT2 inhibitor AGK2 (10 μM) or control DMSO, and cell proliferation was monitored. Quantitative results are shown (n=5).

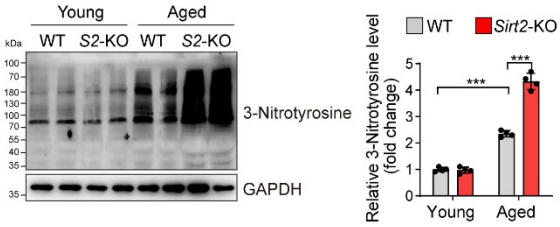

Supplementary Figure 5. SIRT2 regulates protein oxidation. Protein oxidation in aged aortas was monitored by 3-Nitrotyrosine with western blot. Representative blots and quantitative results are shown (n=4). Statistical analysis was performed using one-way ANOVA with Bonferroni *post hoc* test. ***p<0.001.

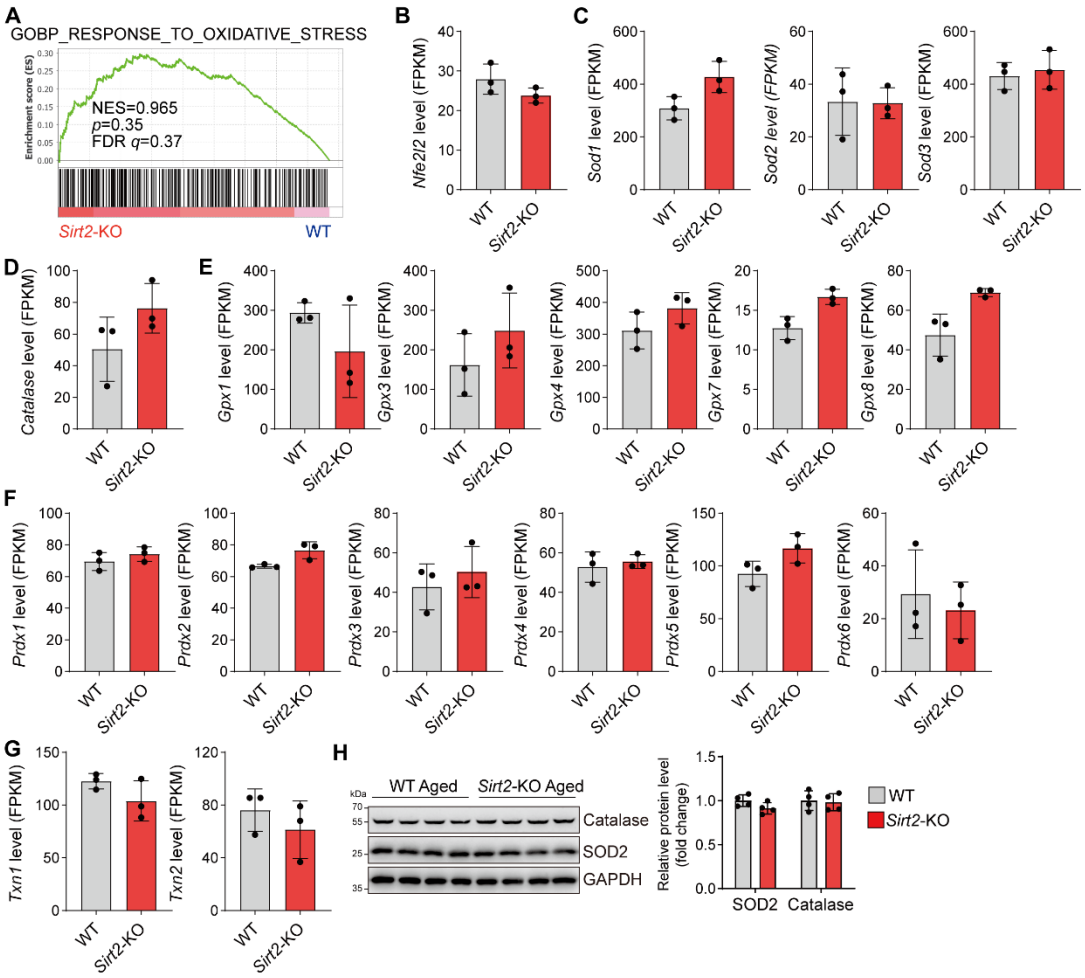

Supplementary Figure 6. SIRT2 does not affect antioxidative enzymes in the aortas. (A) Gene set enrichment analysis revealing SIRT2 does not affect the antioxidative signal in aged aortas. (B-G) Transcriptome (bulk RNA-seq data) of young and aged aortas shows comparable expressions of antioxidants in aged WT and *Sirt2*-KO aortas, including antioxidative transcriptional factor Nrf2 (B), Sod (C), Catalase (D), Gpx (E), Prdx (F), Txn (G). (H) Western blot analysis of SOD2 and Catalase in aged WT and *Sirt2*-KO aortas. Representative blots and quantitative results are shown (n=4).

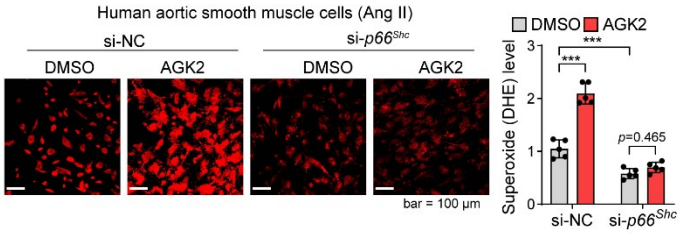

Supplementary Figure 7. p66^{Shc} regulates oxidative stress in human vascular cells. Aortic smooth muscle cells were transfected with si-*p66^{Shc}* or control si-NC for 24 h, followed by treatment with or without the SIRT2-specific inhibitor AGK2 (10 μM) and angiotensin II (Ang II, 1 μM) for another 24 h. Total superoxide levels were monitored by DHE staining (n=4). Statistical analyses were performed using one-way ANOVA with Bonferroni *post hoc* test. ***p<0.001.

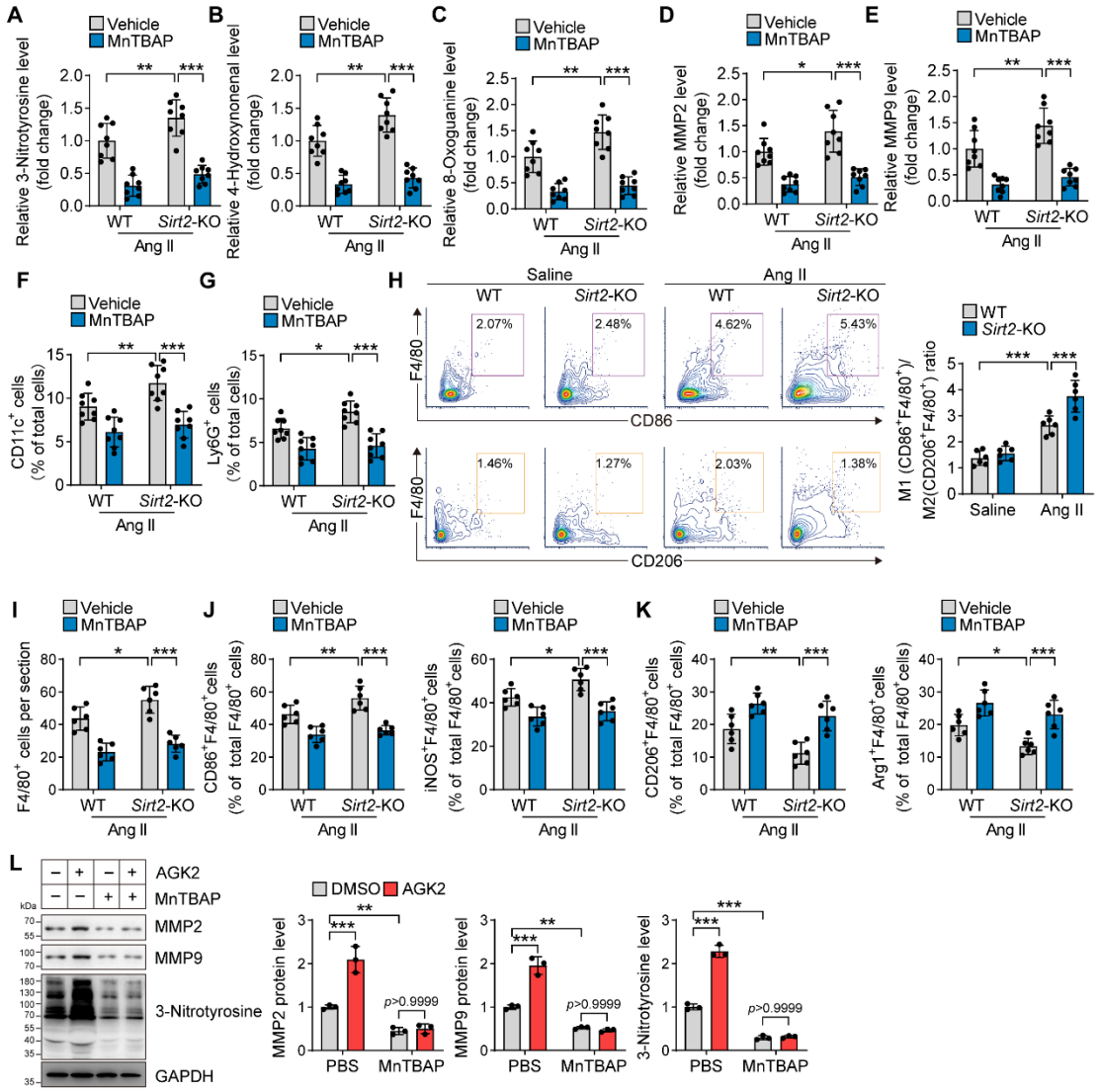

Supplementary Figure 8. MnTBAP regulates SIRT2 effects on vascular remodelling induced by angiotensin II. (A-C) *Sirt2* deficiency promotes protein oxidation (A), lipid peroxidation (B) and DNA oxidation (C) in the aortas of angiotensin II (Ang II)-infused mice, which was blocked by MnTBAP treatment. Quantitative results are shown (n=8). Male young (4-month-old) WT and *Sirt2*-knockout (*Sirt2*-KO) mice were infused with Ang II (1.3 mg/kg/day) to replicate vascular ageing phenotypes. The mice were also treated with/without the superoxide scavenger MnTBAP (5 mg/kg/day, i.p.) treatment for 4 weeks. (D-E) MnTBAP treatment blocks the effects of *Sirt2* deficiency on MMP2 and MMP9 expression in the aortas of Ang II-infused mice. Quantitative results are shown (n=8). (F-G) MnTBAP treatment blocks the effects of *Sirt2* deficiency on the infiltration of dendritic cells (F), and neutrophils (G) in the aortas of Ang II-infused mice. Quantitative results are shown (n=8). (H-K) SIRT2 regulated macrophage polarisation. (H) FACS results showing *Sirt2* deficiency promotes macrophages toward pro-inflammatory M1 phenotype in aortas of Ang II-infused mice (n=6). (I) Immunostaining revealing that MnTBAP treatment blocks the effects of *Sirt2* deficiency on total macrophage ($F4/80^+$) in aortas of Ang II-infused mice (n=6). (J) Immunostaining revealing that MnTBAP treatment blocks the effects of *Sirt2* deficiency on M1 macrophage ($CD86^+F4/80^+$ and $iNOS^+F4/80^+$) polarisation in aortas of Ang II-infused mice (n=6). (K) Immunostaining revealing that MnTBAP treatment blocks the effects of *Sirt2* deficiency on M2 macrophage polarisation

($CD206^+F4/80^+$ and $Arg1^+F4/80^+$) in aortas of Ang II-infused mice (n=6). (L) Reactive oxygen species contributed to SIRT2 function in regulating protein oxidation and MMP expression in aortic smooth muscle cells (ASMCs). ASMCs were treated with MnTBAP (10 mM) in the presence/absence of SIRT2-specific inhibitor AGK2 (10 μM) and Ang II (1 μM) for another 24 hours. Protein expression was analysed by western blot. Representative blots and quantitative results are shown (n=3). MMP, matrix metalloprotein. Statistical analyses were performed using one-way ANOVA with Bonferroni *post hoc* test. **p*<0.05, ***p*<0.01, ****p*<0.001.

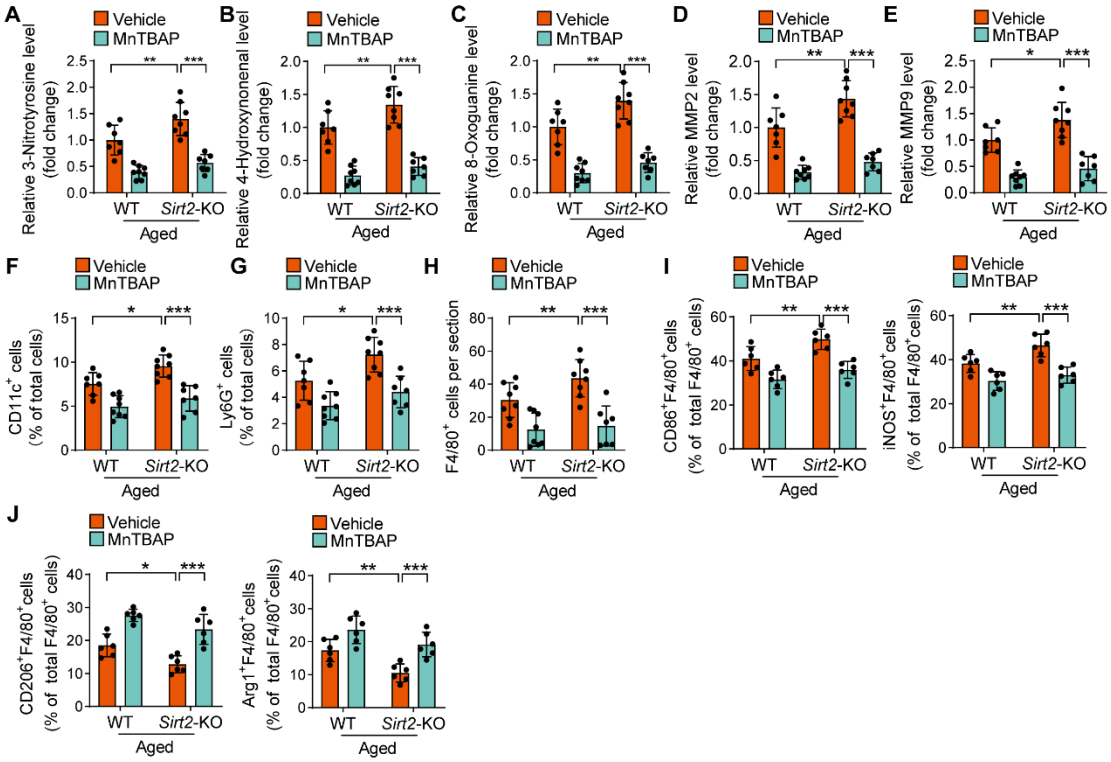

Supplementary Figure 9. MnTBAP regulates SIRT2 effects on vascular remodelling induced by ageing. (A-C) *Sirt2* deficiency promotes protein oxidation (A), lipid peroxidation (B) and DNA oxidation (C) in aged aortas, which is blocked by MnTBAP treatment. Quantitative results are shown (n=7–8). (D-E) MnTBAP treatment blocks the effects of *Sirt2* deficiency on MMP2 and MMP9 expression in aged aortas (n=7–8). (F-G) MnTBAP treatment blocks the effects of *Sirt2* deficiency on the infiltration of dendritic cells (F), and neutrophils (G) in the aortas of aged mice. Quantitative results are shown (n=7-8). (H-J) SIRT2 regulates macrophage polarisation. (H) Immunostaining revealing that MnTBAP treatment blocks the effects of *Sirt2* deficiency on total macrophage ($F4/80^+$) in the aortas of aged mice (n=6). (I) Immunostaining revealing that MnTBAP treatment blocks the effects of *Sirt2* deficiency on M1 macrophage ($CD86^+F4/80^+$ and $iNOS^+F4/80^+$) polarisation in aortas of aged mice (n=6). (J) Immunostaining revealing that MnTBAP treatment blocks the effects of *Sirt2* deficiency on M2 macrophage polarisation ($CD206^+F4/80^+$ and $Arg1^+F4/80^+$) in aortas of aged mice (n=6). Statistical analyses were performed using one-way ANOVA with Bonferroni *post hoc* test. **p*<0.05, ***p*<0.01, ****p*<0.001.

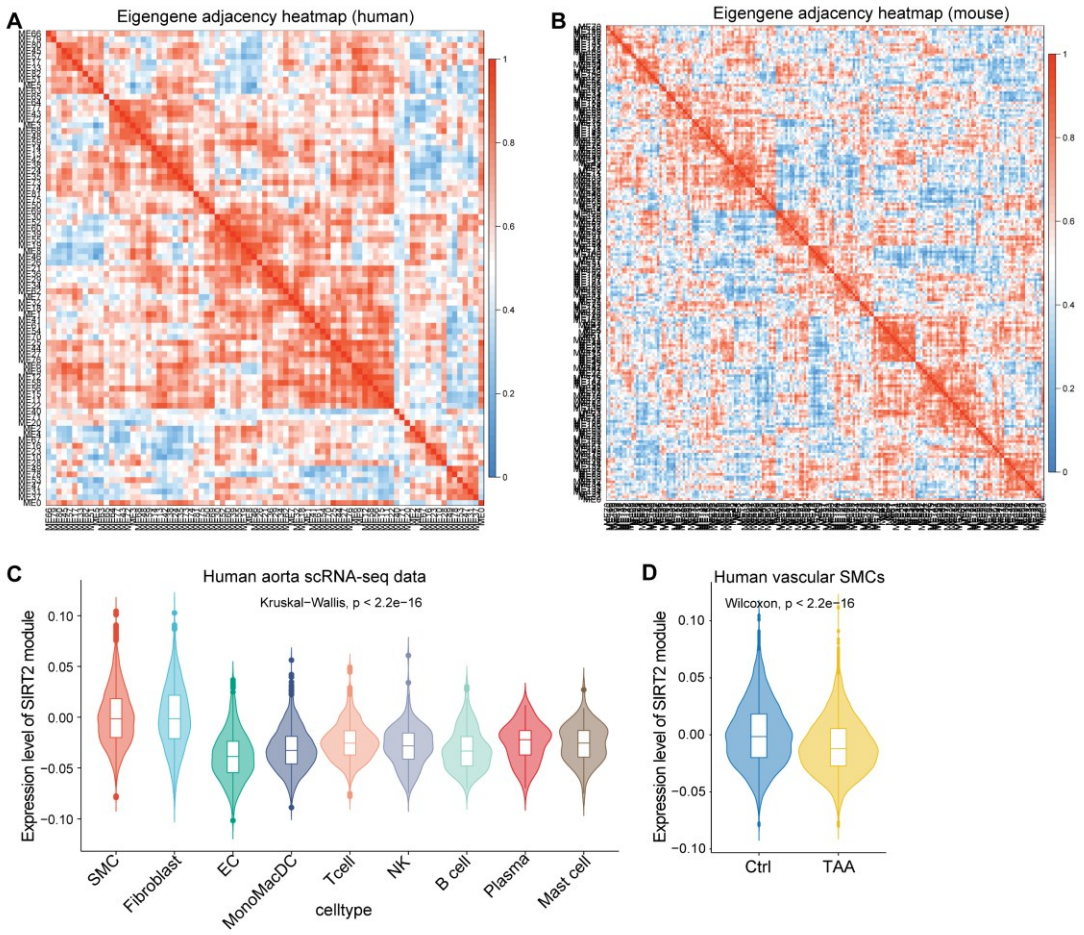

Supplementary Figure 10. Analysis of SIRT2-coexpressing module in human and mouse aortas. (A) Eigengene adjacency heatmap of human aortas. (B) Eigengene adjacency heatmap of mouse aortas. (C) Expression of SIRT2-coexpressing module in human aortic samples at the single cell level. EC, endothelial cell; Mono, monocyte; Mac, macrophage; DC, dendritic cell; NK, natural killer cell. (D) Expression of SIRT2-coexpressing module in SMCs from human control and thoracic aortic aneurysm (TAA) aortic samples. Statistical analyses were performed using the Kruskal-Wallis test (C) and Wilcoxon test (D).

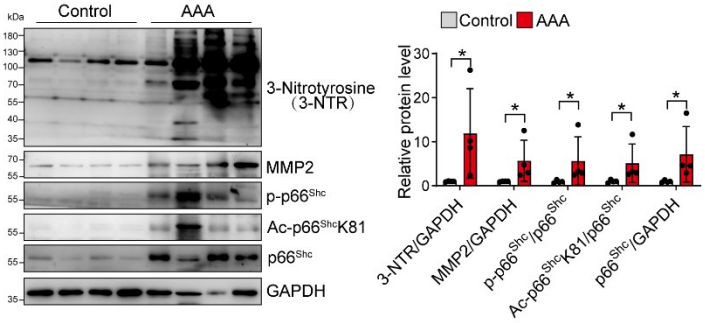

Supplementary Figure 11. p66^{Shc} acetylation/activation and oxidative stress in human aortic tissues. p66^{Shc} acetylation/activation and oxidative stress in human AAA. Western blot was performed to evaluate the expression of total p66^{Shc}, p66^{Shc} phosphorylation, p66 acetylation (K81), MMP2 expression as well as protein oxidation (3-Nitrotyrosine) in the human abdominal aortic aneurysm (AAA) and control aortic tissues (n=4). Statistical analyses were performed using the Mann-Whitney test. *p<0.05.